Multiscale Modelling of Norovirus

Maphiri A.D

Department of Mathematical and Computational Sciences
Faculty of Science, Engineering and Agriculture
University of Venda

SAMS PRESENTATION

Supervisor: Prof W.Garira
Co-Supervisor: Prof D. Mathebula
Co-Supervisor: Dr K.Muzhinji

December 7, 2022

Outline

Introduction

- Norovirus is one of the most causes of infectious diseases.
- *Norovirus* is one of the most common causes of gastroenteritis around the world due to its multiple transmission routes, and primary cause of both sporadic and epidemic gastroenteritis, as well as being very contagious.
- It is the most frequent cause of food poisoning, community-acquired diarrhea, and gastroenteritis in people of all ages.
- It is estimated that 19–21 million cases of acute gastroenteritis are caused by *noroviruses* annually in the USA, resulting in 56000–71000 hospitalizations, 1.7–1.9 million outpatient visits, 400000 emergency department visits, 570–800 deaths, predominantly in old and young patients.
- Hospitalizations associated with the *noroviruses* in the USA have resulted in a 500 million financial burden.

- As of today, no vaccines or specific treatments are available, except palliative treatment (good sanitation, personal hygiene practices, and isolation or quarantine) to control the spread of the disease.
- The primary route is fecal-oral, which occurs mainly through by ingestion of contaminated food or water or person-to-person contact.
- Mathematical models have proven instrumental in preventing and controlling most emerging infectious diseases, such as SARS, HIV/AIDS, H5N1, and H1N1
- Most frequently, systems of nonlinear ordinary differential equations are used to characterize these models.
- Since epidemic spread typically causes great trauma to society, accurate mathematical models of infectious disease propagation are useful in analyzing the detailed spreading process.
- Hence, it is absolutely crucial to establish propagation models that are accurate while taking infection spreading issues into account.

- Traditional approaches for modelling infectious diseases have, until recently, been focusing on describing key disease processes within-host (microscale) and between-host (macroscale) separately using single-scale models
- Since pathogens multiply within hosts, spread across people, and infect entire populations of hosts, infectious disease systems are essentially multiscale complex systems.
- Multiscale modelling is a modelling technique that describes a system by simultaneously using many models at various scales.
- Multiscale modeling of infectious disease systems takes into account a number of factors, amongst others:
  - It examines the progression of infectious diseases at the level of infection,
  - It adresses the need to study factors that influence disease dynamics, such as immune response, health interventions, and environmental changes,
  - It includes more details in infectious disease system modeling, and reduce modeling errors in those systems

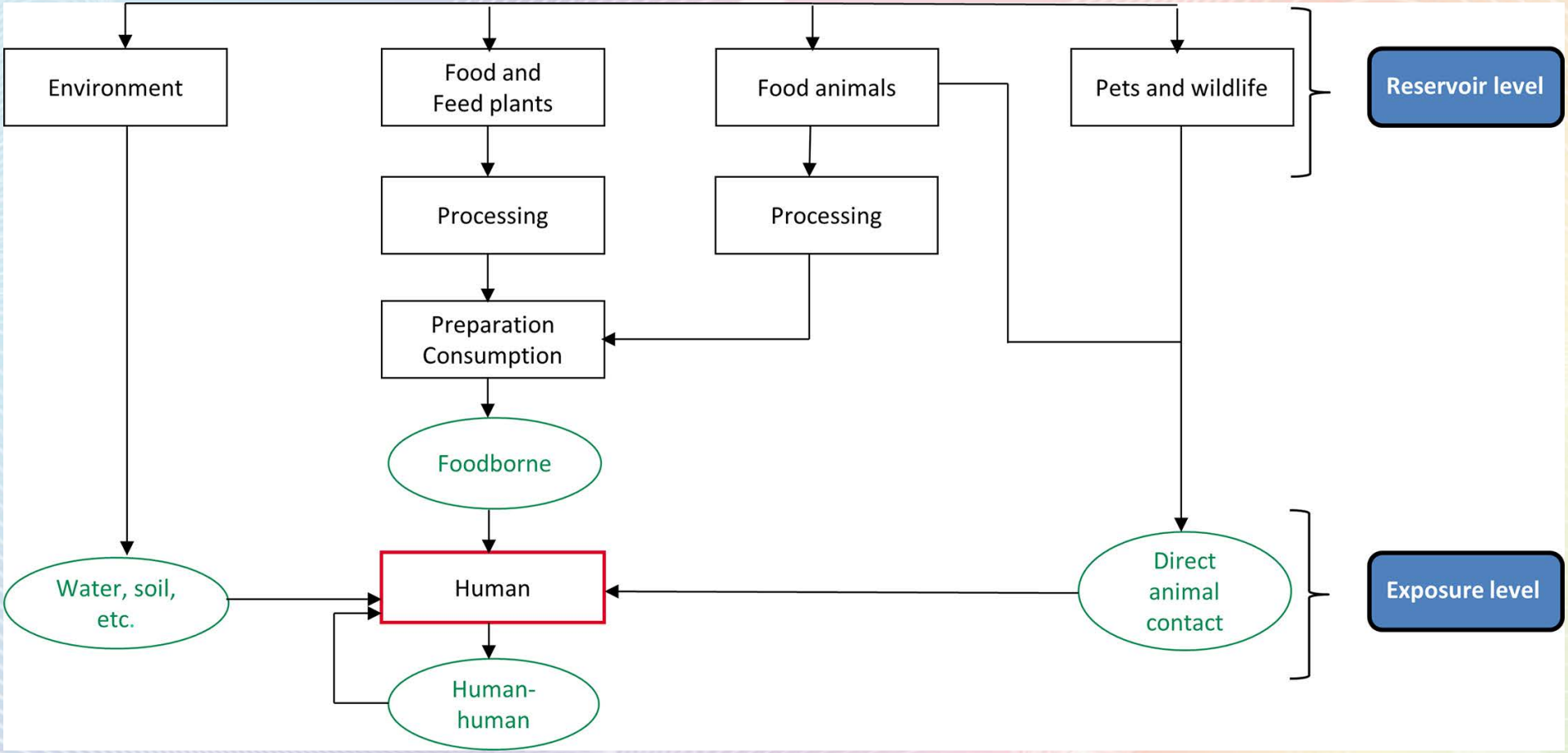

FIGURE 1: Major transmission routes of human foodborne diseases illustrating two points of attribution: the reservoir level and exposure level .

- The complex disease system is conceptualized as being organized into seven main fundamental hierarchical levels such as cell, tissue, organ, microecosystem, host, community and macrosystem levels.
- Furthermore, each of these levels can further be subdivided into connected scales which are the individual/lower/microscale and population/upper/macroscale. Below is a summary of these levels and their scales:

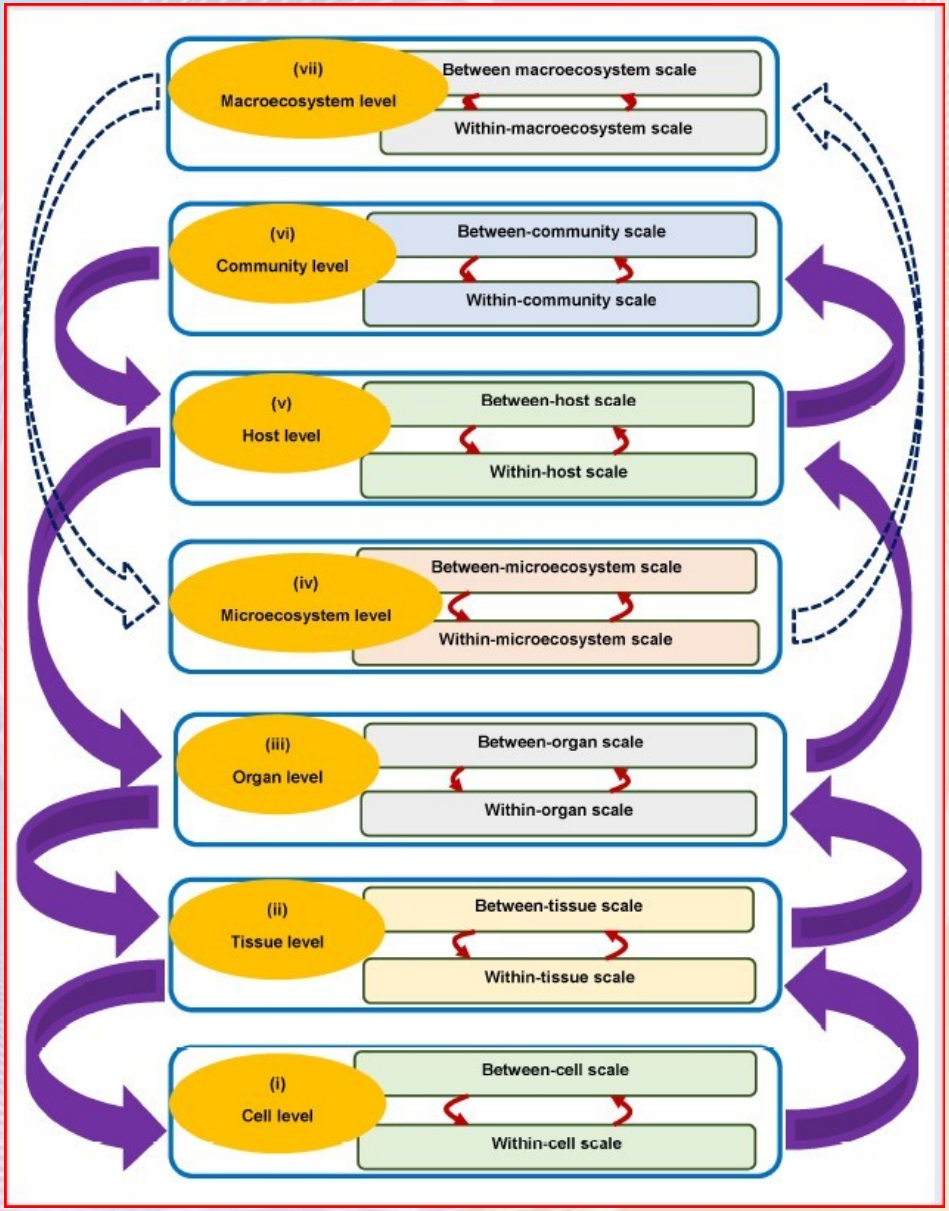

FIGURE 2: The seven hierarchical levels of organisation of infectious disease dynamics

- At each of these seven hierarchical levels, five distinct categories of multiscale models of infectious disease system can be developed that integrate the microscale and macroscale.
  - Individual-based multiscale models (IMSMs),);
  - Nested multiscale models (NMSMs);
  - Hybrid multiscale models (EMSMs);
  - Embedded multiscale models (HMSMs);
  - Coupled multiscale models (CMSMs).

Problem statement

- Studying disease evolution requires an understanding of the interactions between parasites, host resources, and host immunity at the microscale level, parasite transmission, host demography, and epidemiology at the macroscale level, and also the links between levels.
- Recently, multiscale modelling of infectious disease systems has begun to receive an overwhelming appreciation as opposed to single-scale modelling.
- Yet, there has been nothing that has been done in attempt to describe and undertand how *norovirus* causes infection in humans using multicale modelling.
- We fill this gap by developing a nested multiscale model that will provide a thorough understanding of complex life of *norovirus*.

Literature Review

- A simple deterministic compartment model to analyse a *norovirus* outbreak in long-term care facilities in a closed population was developed in (2009), the model has shown necessity to improved infection control measures.
- An age-structured deterministic model for transmission aimed to assess the duration of immunity after infection, and the age-dependence of transmission was developed in 2013.
- In 2015, Lopman developed a dynamic transmission model of *norovirus* infection, disease and immunity in a way to advance an understanding of the high prevalence of asymptomatic infection.
- A simulation model to determine the potential cost-savings from the hospital perspective of implementing various *norovirus* outbreak control interventions was constructed in 2011.
- However all these models are single scales models, thus they focus on macroscale only without considering the effect of the microscale dynamics.

- There are exististing multiscale models frameworks for infectious diseases such as guinea worm (Netshikweta & Garira,2017), vector-borne (Mathebula, 2018) and malaria (Garira & Mathebula, 2019).
- Therefore, this study is the first of its kind to use nested multiscale model catergory in describing and understanding the complex life-cycle of *norovirus*

Overall Aim

Main Aim

- The main aim is to develop a nested multiscale model to describe and understand the dynamics of *norovirus*.

Objective

- To develop microscale submodel and macroscale submodel and integrate them to form a multiscale model of *norovirus*.

A Nested Multiscale Model of *Norovirus*

Present a nested multiscale model for *Norovirus*

- That integrates two adjacent scales at a host level of the disease.

Key feature of nested multiscale models

- The most important feature of nested multiscale models at any level of organization of an infectious disease system is that the macroscale influences the microscale through the initial infective inoculum and microscale influences macroscale through pathogen excretion/shedding.

The macroscale *NOROVIRUS* transmission sub-model assumptions

I. The transmission of the infection is only through contact with bacterial load (V_H) in the physical environment. However, if there is any direct transmission, it can be estimated by indirect transmission in terms of environmental viral load (V_H).

II. The dynamics of S_H, I_H and V_H are assumed to occur at slow time scale, t, compared to the within-host scale *norovirus* transmission dynamics variables so that $S_H = S_H(t)$, $I_H = I_H(t)$ and $V_H = V_H(t)$.

III. The average virus in each infected human is modelled phenomenologically by $\widehat{N}_h$, which is a proxy for individual human infectiousness.

IV. The environmental *norovirus* (V_H) do not replicate in the environment (outside-host).

Derivation of nested multiscale model of *NOROVIRUS* transmission dynamics

1. The macroscale transmission submodel:

$$
\begin{cases}
1. \ \dfrac{dS_H(t)}{dt} = \Lambda_H - \dfrac{\beta_H S_H V_H}{P_0 + V_H} - \mu_H S_H, \\
2. \ \dfrac{dI_H(t)}{dt} = \dfrac{\beta_H S_H V_H}{P_0 + V_H} - (\delta_H + \mu_H) I_H, \\
3. \ \dfrac{dV_H(t)}{dt} = \widehat{N_h} \alpha_h I_H - \mu_V V_H.
\end{cases} \tag{1}
$$

The microscale *NOROVIRUS* transmission submodel assumptions

I. Transmission of the infection at microscale is only through contact with the viral load B_h at the site of infection.

II. The microscale disease process happen at fast time scale, τ, compared to the macroscale *norovirus* submodel variable so that $B_h = B_h(\tau)$, $S_e = S_e(\tau)$, $I_e = I_e(\tau)$, and $I_c = I_c(\tau)$.

III. The microscale viral load modelled mechanistically by $B_h = B_h(\tau)$ is a proxy for individual human infectiousness.

IV. The virus replicate in the epithelial cells of an individual human.

1. The microscale transmission submodel:

$$
\begin{cases}
1. \ \dfrac{dB_h(\tau)}{d\tau} = N_e\alpha_e I_e(\tau) - \phi_t I_c B_h(\tau) - \mu_h B_h(\tau) - \alpha_h B_h(\tau), \\
2. \ \dfrac{dS_e(\tau)}{d\tau} = \Lambda_e - \beta_e S_e B_h(\tau) - \mu_e S_e(\tau), \\
3. \ \dfrac{dI_e(\tau)}{dt} = \beta_e S_e B_h(\tau) - \mu_e I_e(\tau) - \alpha_e I_e(\tau), \\
4. \ \dfrac{dI_c(\tau)}{d\tau} = \Lambda_c + \rho_c I_c B_h(\tau) - \mu_c I_c(\tau).
\end{cases} \tag{2}
$$

Integrating the macroscale and microscale submodels

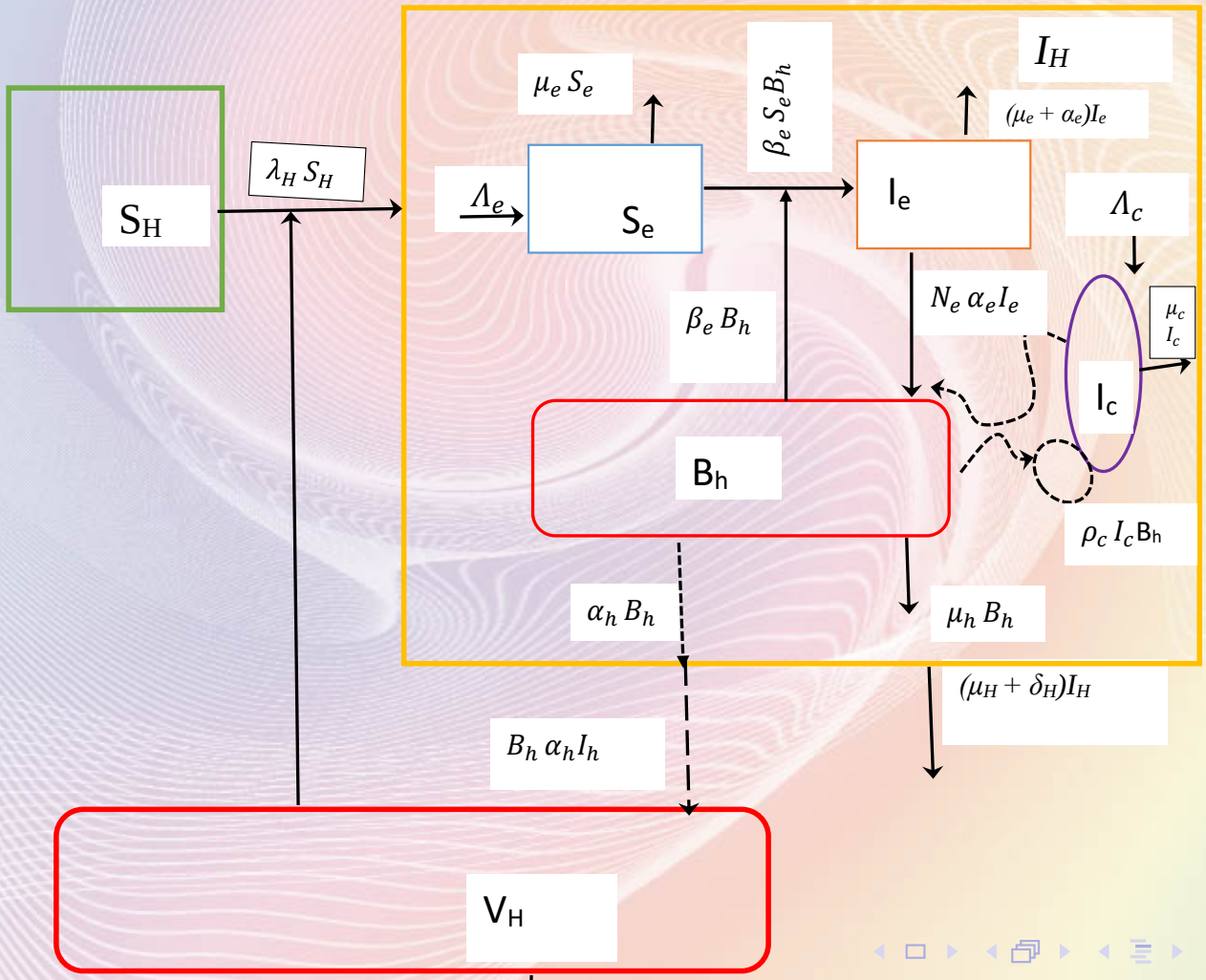

Simplified Multiscale Model For *Norovirus*

A Full Nested Multiscale Model:

$$
\begin{cases}
1.\ \dfrac{dS_H(t)}{dt} = \Lambda_H - \dfrac{\beta_H S_H V_H}{P_0+V_H} - \mu_H S_H(t), \\
2.\ \dfrac{dI_H(t)}{dt} = \dfrac{\beta_H S_H V_H}{P_0+V_H} - (\delta_H + \mu_H) I_H(t), \\
3.\ \dfrac{dV_H(t)}{dt} = \alpha_h B_h(\tau) I_H(t) - \mu_V V_H(t), \\
4.\ \dfrac{dB_h(\tau)}{d\tau} = N_e \alpha_e I_e(\tau) - \phi_t I_c B_h(\tau) - \mu_h B_h(\tau) - \alpha_h B_h(\tau), \\
5.\ \dfrac{dS_e(\tau)}{d\tau} = \Lambda_e - \beta_e S_e B_h(\tau) - \mu_e S_e(\tau), \\
6.\ \dfrac{dI_e(\tau)}{dt} = \beta_e S_e B_h(\tau) - \mu_e I_e(\tau) - \alpha_e I_e(\tau), \\
7.\ \dfrac{dI_c(\tau)}{d\tau} = \Lambda_c + \rho_c I_c B_h(\tau) - \mu_c I_c(\tau).
\end{cases} \tag{3}
$$

Fast-slow time-scale method

- Assuming a relation between the fast, τ and slow time-scales, t to be of the form $t = \epsilon\tau$:

The Full Nested Multiscale Model Become:

$$
\begin{cases}
1.\ \frac{dS_H(t)}{dt} = \Lambda_H - \frac{\beta_H S_H V_H}{P_0+V_H} - \mu_H S_H(t), \\
2.\ \frac{dI_H(t)}{dt} = \frac{\beta_H S_H V_H}{P_0+V_H} - (\delta_H + \mu_H) I_H(t), \\
3.\ \frac{dV_H(t)}{dt} = \alpha_h B_h(\tau) I_H(t) - \mu_V V_H(t), \\
4.\ \epsilon\frac{dB_h(\tau)}{d\tau} = N_e \alpha_e I_e(\tau) - \phi_t I_c B_h(\tau) - \mu_h B_h(\tau) - \alpha_h B_h(\tau), \\
5.\ \epsilon\frac{dS_e(\tau)}{d\tau} = \Lambda_e - \beta_e S_e B_h(\tau) - \mu_e S_e(\tau), \\
6.\ \epsilon\frac{dI_e(\tau)}{dt} = \beta_e S_e B_h(\tau) - \mu_e I_e(\tau) - \alpha_e I_e(\tau), \\
7.\ \epsilon\frac{dI_c(\tau)}{d\tau} = \Lambda_c + \rho_c I_c B_h(\tau) - \mu_c I_c(\tau).
\end{cases} \tag{4}
$$

Estimation of $\widehat{N}_h$ from the Full Nested Multiscale Model

- Setting ϵ to zero, then the within-host scale submodel becomes independent of time and we obtain:

$$\begin{cases} 1.\ N_e\alpha_e I_e^* - \phi_t I_c^* - B_h^* - \mu_h B_h^* - \alpha_h B_h^* = 0, \\ 2.\ \Lambda_e - \beta_e S_e^* B_h^* - \mu_e S_e^* = 0, \\ 3.\ \beta_e S_e^* B_h^* - \mu_e I_e^* - \alpha_e I_e^* = 0, \\ 4.\ \Lambda_c + \rho_c I_c^* B_h^* - \mu_c I_c^* = 0. \end{cases} \tag{5}$$

Estimation of $\widehat{N}_h$ from the Full Nested Multiscale Model Continues....

$$
\begin{cases}
B_h^* &= \dfrac{b_1 + \sqrt{b_1^2 + 4b_0 b_2}}{2b_0}, \\
b_0 &= \beta_e \rho_c (\mu_c + \alpha_e)(\mu_h + \alpha_h), \\
b_1 &= (\mu_e + \alpha_e)(\beta_e a_0 - \mu_e a_1) + N_e \alpha_e \Lambda_e \beta_e \rho_c, \\
b_2 &= Ne \alpha_e \Lambda_e \mu_c - a_2 \mu_c (\mu_e + \alpha_e), \\
a_0 &= \phi_t \Lambda_c + \mu_h \mu_e + \alpha_h \mu_c, \\
a_1 &= (\mu_h + \alpha_h)\rho_c, \\
a_2 &= \phi_t \Lambda_c + (\mu_h + \alpha_h)\mu_c.
\end{cases} \tag{6}
$$

Estimation of $\widehat{N}_h$ from the Full Nested Multiscale Model Continue....

- The total number of microscale viral excreted outside the host $B_h I_H$ is now approximated by $B_h^* I_H$.
- Using the notation that $N_h = B_h^*$, the macroscale submodel dynamics becomes:

$$\begin{cases} 1. \ \frac{dS_H(t)}{dt} = \Lambda_H - \frac{\beta_H S_H V_H}{P_0 + V_H} - \mu_H S_H, \\ 2. \ \frac{dI_H(t)}{dt} = \frac{\beta_H S_H V_H}{P_0 + V_H} - (\delta_H + \mu_H) I_H, \\ 3. \ \frac{dV_H(t)}{dt} = N_h \alpha_h I_H - \mu_V V_H. \end{cases} \tag{7}$$

Estimation of $\widehat{N}_h$ from the Full Nested Multiscale Model Continue....

- The composite parameter N_h which estimates $\widehat{N}_h$ is given by:

$$\begin{cases} N_h &= \dfrac{b_1 + \sqrt{b_1^2 + 4b_0b_2}}{2b_0}, \\ b_0 &= \beta_e\rho_c(\mu_c + \alpha_e)(\mu_h + \alpha_h), \\ b_1 &= (\mu_e + \alpha_e)(\beta_e a_0 - \mu_e a_1) + N_e\alpha_e\Lambda_e\beta_e\rho_c. \\ b_2 &= a_2\mu_c(\mu_e + \alpha_e)(R_0 - 1) \\ a_0 &= \phi_t\Lambda_c + \mu_h\mu_e + \alpha_h\mu_c, \\ a_1 &= (\mu_h + \alpha_h)\rho_c, \\ a_2 &= \phi_t\Lambda_c + (\mu_h + \alpha_h)\mu_c. \end{cases} \tag{8}$$

Mathematical Analysis of the Simplified Nested Multiscale Model

Mathematical analysis of the properties for the *norovirus* nested multiscale model is conducted in the region $\Omega_1 \in \mathbb{R}^+_3$ of biological interest which is given by the feasible set for our multiscale model system (7) is given by

Invariant region

$$\begin{cases} \Omega_1 = (S_H(t), I_H(t), V_H(t)) \in \mathbb{R}^+_3 : \\ \qquad 0 \leq S_H + I_H \leq \frac{\Lambda_H}{\mu_H}, \quad 0 \leq V_H \leq \frac{N_h \alpha_h \Lambda_H}{\mu_H \mu_V}, \end{cases} \tag{9}$$

The basic reproductive number (R_0)

R_0, is the expected number of secondary cases produced, in a completely susceptible population, by a typical infective individual. If $R_0 < 1$, then on average an infected individual produces less than one new infected individual over the course of his infectious period, and the infection cannot grow. Conversely, if $R_0 > 1$, then each infected individual produces, on average, more than one new infection, and the disease can invade the population.

$$\begin{cases} R_0 = R_{0_{WH}} R_{0_{BH}} = \dfrac{N_h \alpha_h \beta_H \Lambda_H}{(\delta_H + \mu_H) P_0 \mu_H \mu_V}, \\ R_{0_{WH}} = \dfrac{N_h \alpha_h}{\mu_H (\mu_H + \delta_H)}, \\ R_{0_{BH}} = \dfrac{\beta_H \Lambda_H}{\mu_V P_0}. \end{cases} \tag{10}$$

Nonstandard finite difference scheme(NSFDS)

The NSFDS overcomes the weaknesses of the traditional numerical schemes such as Runge-Kutta and Euler methods where it depends on the two main rules. First, the denominator function should be replaced by $0 < \phi(h) < 1$, Second, the nonlinear terms right-hand side are approximated in a nonlocal way. We present a NSFDS for Model (7). We discretise the time variable to $t_k = kh$ for $k = 0, 1, 2$ and a constant h, where $h > 0$.

$$\begin{cases} 1.\ \frac{S_H^{k+1}-S_H^k}{\phi_1(h)} = \Lambda_H - \frac{\beta_H S_H^{k+1} V_H^k}{P_0+V_H^k} - \mu_H S_H^{k+1}, \\ 2.\ \frac{I_H^{k+1}-I_H^k}{\phi_2(h)} = \frac{\beta_H S_H^{k+1} V_H^k}{P_0+V_H^k} - (\delta_H + \mu_H) I_H^{k+1}, \\ 3.\ \frac{V_H^{k+1}-V_H^k}{\phi_3(h)} = N_h \alpha_h I_H^{k+1} - \mu_V V_H^{k+1}. \end{cases} \tag{11}$$

$$\begin{cases} \phi_1(h) &= \frac{e^{h\mu_H}-1}{\mu_H}, \\ \phi_2(h) &= \frac{e^{h(\mu_H+\delta_H)}-1}{\mu_H+\delta_H}, \\ \phi_3(h) &= \frac{e^{h\mu_V}-1}{\mu_V}. \end{cases}$$

Rearranging equation (11) we obtain:

$$\begin{cases} 1.\ S_H^{k+1} = \dfrac{\phi_1(h)\Lambda_H + S_H^k}{1+\phi_1(h)\left[\frac{\beta_H V_H^k}{P_0+V_H^k}+\mu_H\right]}, \\ 2.\ I_H^{k+1} = \dfrac{I_H^k+\phi_2(h)\left[\frac{\beta_H V_H^k S_H^{k+1}}{P_0+V_H^k}\right]}{1+\phi_2(h)(\delta_H+\mu_H)}, \\ 3.\ V_H^{k+1} = \dfrac{\phi_3(h)N_h\alpha_h I_H^{k+1} + V_H^k}{1+\phi_3(h)\mu_V}. \end{cases} \tag{12}$$

The model focuses on the human population and concentration of *norovirus* in the environment. Therefore, it should be guaranteed that the proposed numerical scheme cannot produce negative values. It can be seen that the proposed numerical scheme produces non-negative values. For the time-step $h > 0$, and $S_H, I_H, V_H > 0$, numerators and denominators are positive and hence $S_H^{k+1}, I_H^{k+1}, V_H^{k+1} > 0$.

Equilibrium Points

We determine the equilibrium points of the numerical scheme by setting $S_H^{k+1} = S_H, I_H^{k+1} = I_H, V_H^{k+1} = V_H$.

$$\begin{cases} 1.\ S_H = \dfrac{\phi_1(h)\Lambda_H + S_H^k}{1+\phi_1(h)\left[\frac{\beta_H V_H^k}{P_0+V_H^k}+\mu_H\right]}, \\ 2.\ I_H = \dfrac{I_H^k+\phi_2(h)\left[\frac{\beta_H V_H^k S_H^{k+1}}{P_0+V_H^k}\right]}{1+\phi_2(h)(\delta_H+\mu_H)}, \\ 3.\ V_H = \dfrac{\phi_3(h)N_h\alpha_h I_H^{k+1} + V_H^k}{1+\phi_3(h)\mu_V}. \end{cases} \tag{13}$$

Equilibrium Points

The disease-free equilibrium point and endemic point are given by:

$E_0 = \left(\frac{\Lambda_H}{\mu_H}, 0, 0\right)$ and $E_1^* = (S_H^*, I_H^*, V_H^*)$ where:

$$\begin{cases} S_H^* &= \frac{\mu_V P_0(\delta_H+\mu_H)(\beta_H+\mu_H)+\mu_H\mu_V P_0(\delta_H+\mu_H)(R_0-1)}{(\beta_H+\mu_H)\beta_H N_h\alpha_h}, \\ I_H^* &= \frac{\mu_h\mu_V P_0(R_0-1)}{N_h\alpha_h(\beta_h+\mu_h)}, \\ V_H^* &= \frac{\mu_H P_0(R_0-1)}{(\beta_H+\mu_H)}. \end{cases} \tag{14}$$

Stabilty Analysis of Equilibrium Points

We use the concept of Jacobian matrix to analyse the stability of the equilibrium points, we define the following function:

$$\begin{cases} f_1(S_H, I_H, V_H) = \frac{S_H^k+\phi_1(h)\Lambda_H(P_0+V_H^k)}{a_3V_H^k+a_1P_0}, \\ , \quad f_2(S_H, I_H, V_H) = \frac{I_H^k(a_3V_H^k+a_1P_0)+\phi_2(h)\beta_H V_H^k[S_H^k+\phi_1(h)\Lambda_H]}{a_2(a_3V_H^k+a_1P_0)}, \\ f_3(S_H, I_H, V_H) = \frac{a_2a_3V_H^{k^2}+V_H^kb_0I_H^k+\phi_2(h)\beta_H(S_H^k+\phi_1(h)\Lambda_H)+I_H^k}{a_2a_4(a_3V_H^k+a_1P_0)}, \end{cases}$$

$$\begin{cases} a_1 &= 1 + \mu_h \phi_1(h), \\ a_2 &= 1 + \phi_2(h)(\delta_H + \mu_H), \\ a_3 &= a_1 + \beta_H \phi_1(h), \\ a_4 &= a_1 + \beta_H \phi_1(h), \end{cases}$$

WE CONSTRUCT THE JACOBIAN MATRIX AS FOLLOWS:

$$J = \begin{bmatrix} J_{11} & J_{12} & J_{13} \\ J_{21} & J_{22} & J_{23} \\ J_{31} & J_{32} & J_{33} \end{bmatrix} \tag{15}$$

where

$$\begin{cases} J_{11} &= \dfrac{P_0+V_H^k}{a_3V_H^k+a_1P_0}, \\ J_{12} &= 0, \\ J_{13} &= \dfrac{(S_H^k+\phi_1(h)\Lambda_H)(a_1-a_3)P_0}{(a_3V_H^k+a_1P_0)^2}, \\ J_{21} &= \dfrac{\phi_2(h)\beta_H V_H^k}{a_2(a_3V_H^k+a_1P_0)}, \end{cases}$$

$$
\begin{cases}
J_{22} &= \frac{a_3 V_H^k + a_1 P_0}{a_2(a_3 V_H^k + a_1 P_0)}, \\
J_{23} &= \frac{a_1 P_0 \phi_2(h)\beta_H(S_H^k + \phi_1(h))\Lambda_H}{a_2(a_3 V_H^k + a_1 P_0)^2}, \\
J_{31} &= \frac{\phi_2(h)\beta_H V_H^k}{a_2 a_4(a_3 V_H^k + a_1 P_0)}, \\
J_{32} &= \frac{\phi_3(h) N_h \alpha_h}{a_2 a_4}, \\
J_{33} &= \frac{b_3(a_3 V_H^k + a_1 P_0)V_H^k + b_4(a_3 V_H^k + a_1 P_0) + b_5(S_H^k + \phi_1(h)\Lambda_H)}{a_2^2 a_4^2(a_3 V_H^k + a_1 P_0)^2}, \\
, \quad b_3 &= a_2^2 a_3 a_4, \\
b_4 &= a_1 a_2^2 a_4 P_0, \\
b_5 &= a_1 a_2 a_4 P_0 \phi_2(h)\beta_H.
\end{cases}
$$

Jacobian matrix at Disease-free Equilibrium Point

$$J(P_0) = \begin{bmatrix} \frac{1}{a_1} & 0 & \frac{\Lambda_H(a_1-a_3)}{\mu_H a_1 P_0} \\ 0 & \frac{1}{a_2} & \frac{\phi_2(h)\beta_H\Lambda_H}{\mu_H a_2 P_0} \\ 0 & \frac{\phi_3(h)N_h\alpha_h}{a_2 a_4} & \frac{\mu_H a_2 P_0+\phi_2(h)\beta_H\Lambda_H}{\mu_H a_2 a_4 P_0} \end{bmatrix} \tag{16}$$

Stability of Diseases-Free Equilibrium Point

We determine the stability of the fixed points of the system (11) numerically.

Time Step	$\rho(\lambda_i)$	NSFD Scheme
0.05	0.9999820	Converges
0.1	0.9999820	Converges
1	0.9999820	Converges
10	0.999820	Converges
100	0.9999820	Converges
1000	0.9999820	Converges

Table 1: The spectral radii of the Jacobian matrix corresponding to the free disease point of NSFD scheme.

Stability of Endemic Equilibrium Point

We will determine the stability of the fixed points of the system (11) numerically.

Time Step	$\rho(\lambda_i)$	NSFD Scheme
0.05	0.9999820	Converges
0.1	0.9999820	Converges
1	0.9999820	Converges
10	0.9999820	Converges
100	0.9999820	Converges
1000	0.9999820	Converges

Table 2: The spectral radii of the Jacobian matrix corresponding to the free disease point of NSFD scheme.

Results:

We note from Table 1 and Table 2 that all the spectral radii are less than one in magnitude irrespective of the time step size used in the simulations.

Hence the disease-free equilibrium $P_0 = \left(\frac{\Lambda_H}{\mu_H}, 0, 0\right)$ for the system when $R_0 < 1$, is unconditionally locally asymptotically stable, and also the endemic equilibrium of the system, is locally asymptotically stable when $R_0 > 1$.

Numerical Simulations:

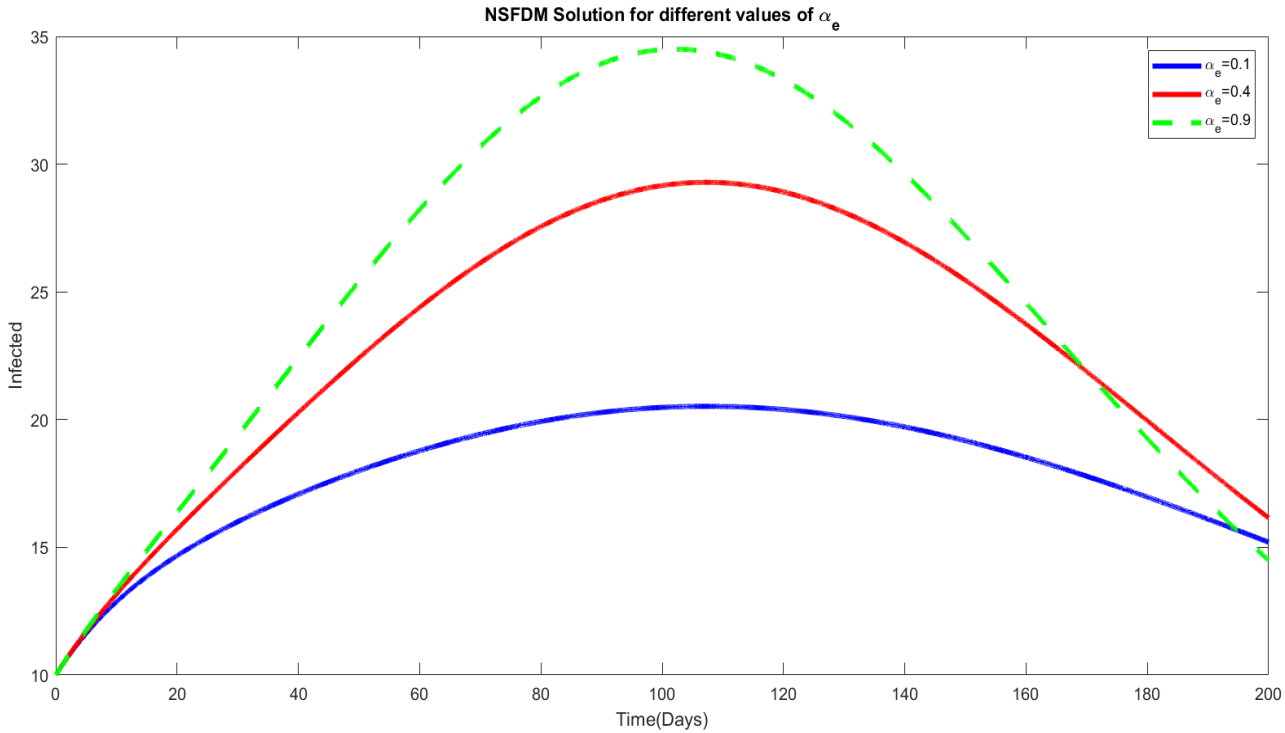

Figure 4: Shows evolution of infected individuals for different values α_e : $\alpha_e = 0.1, \alpha_e = 0.04$ and $\alpha_e = 0.9$.

Numerical Simulations Continue.....

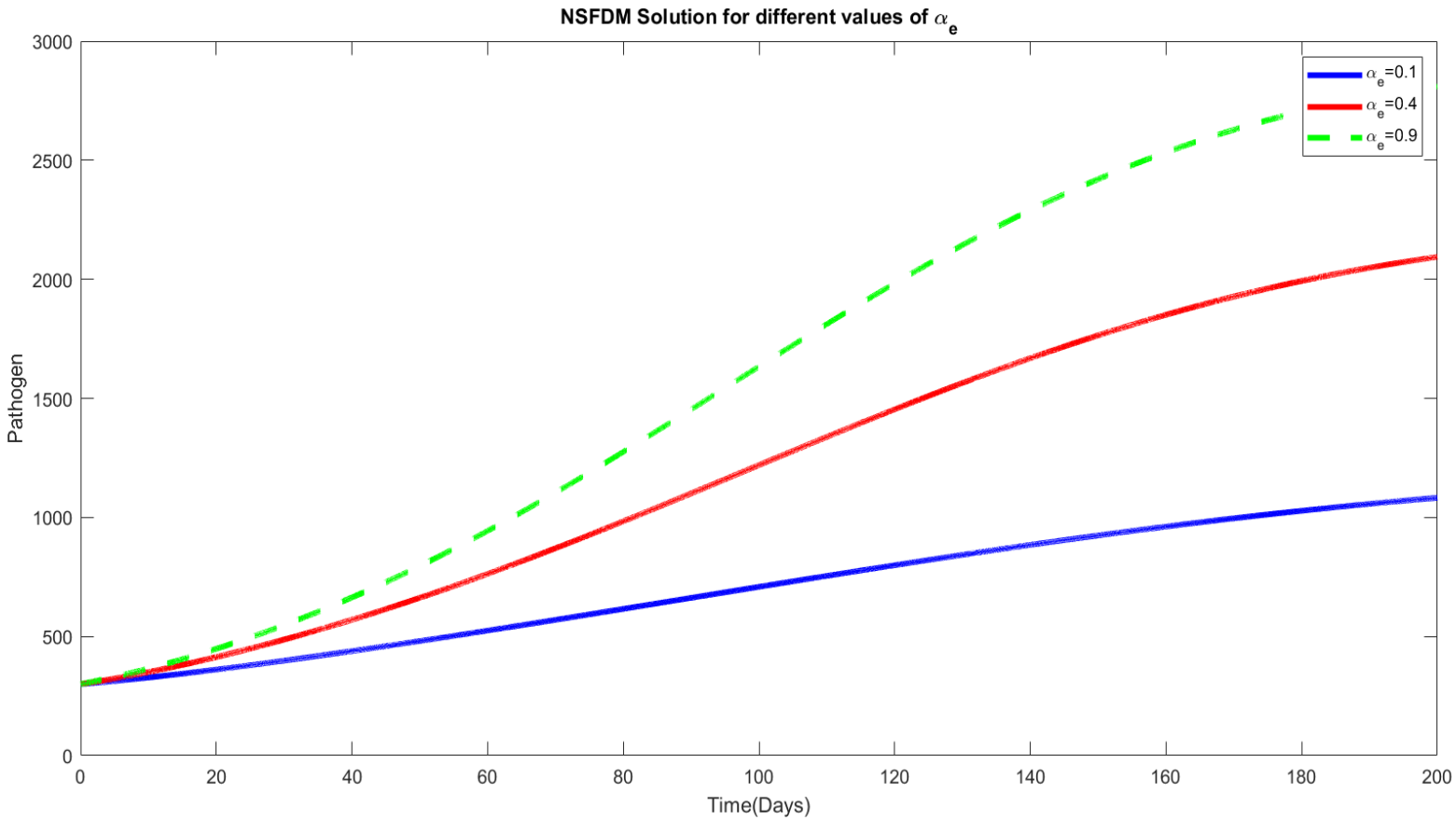

Figure 5: Shows evolution of pathogen in the environment for different values $\alpha_e : \alpha_e = 0.1, \alpha_e = 0.04$ and $\alpha_e = 0.9$.

Numerical Simulations Continue.....

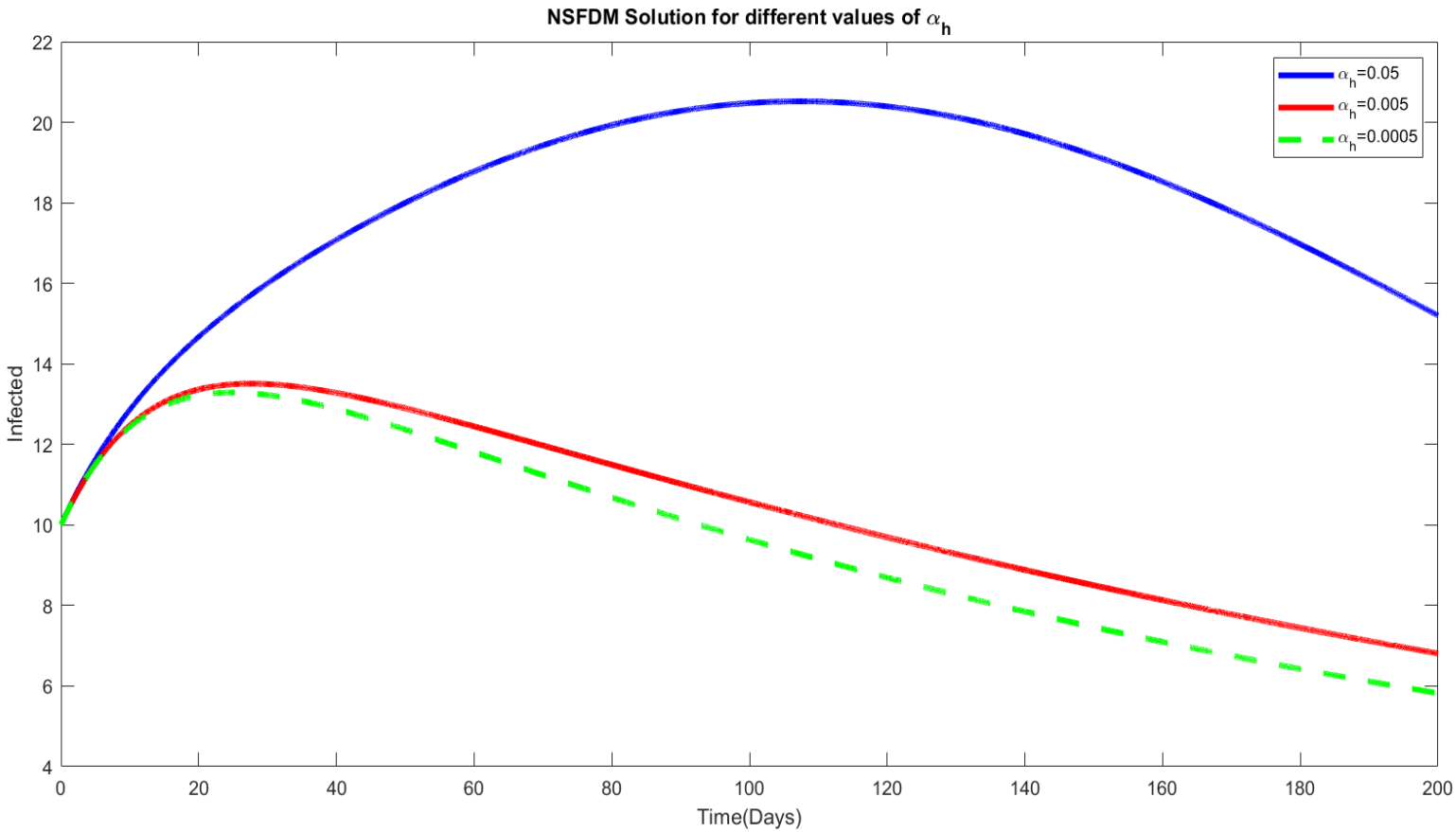

Figure 6: Shows evolution of infected individuals for different values α_h : $\alpha_h = 0.05, \alpha_h = 0.005$ and $\alpha_h = 0.0005$.

Numerical Simulations Continue.....

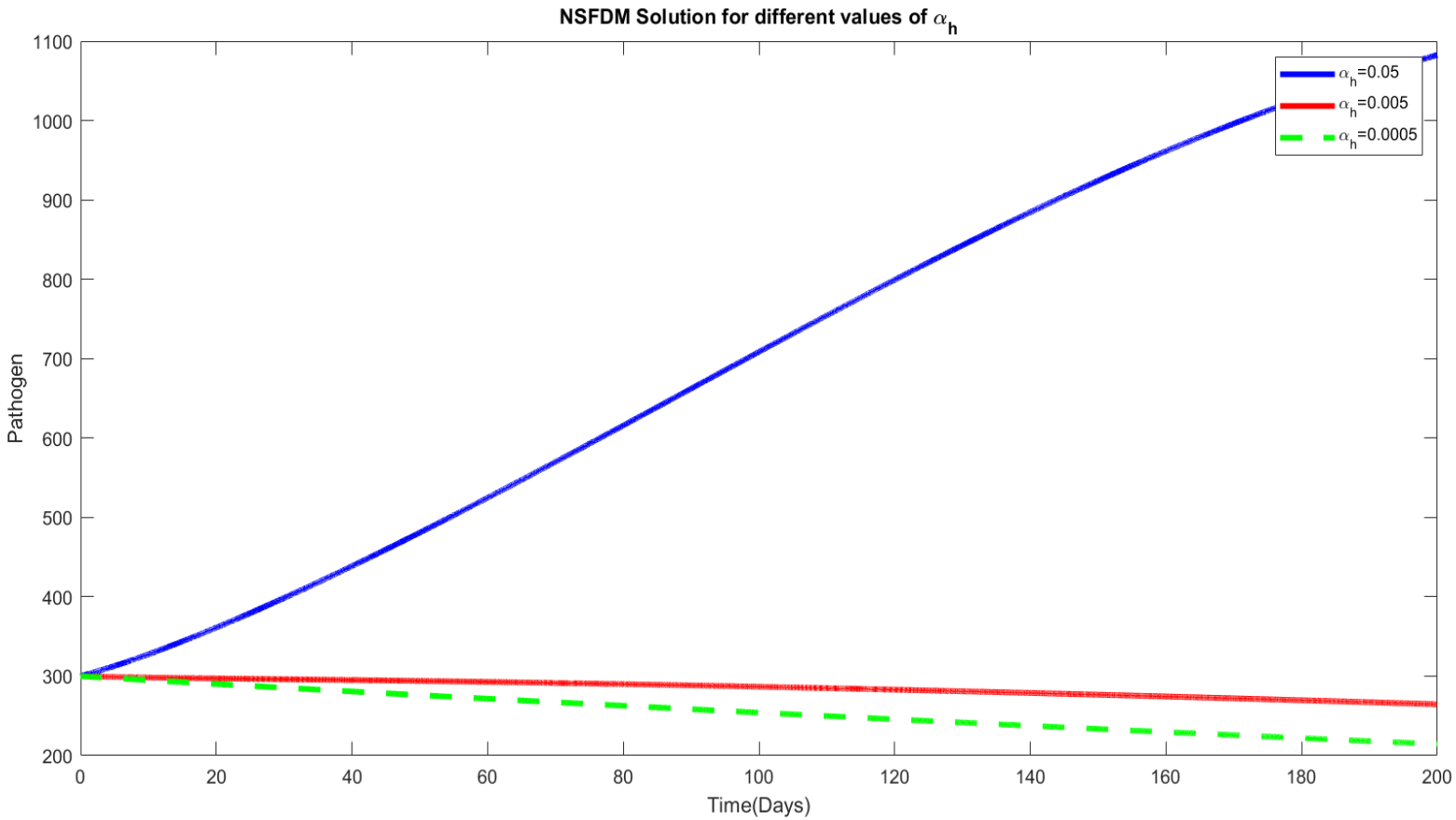

Figure 7: Shows evolution of pathogen in the environment for different values α_h : $\alpha_h = 0.05, \alpha_h = 0.005$ and $\alpha_h = 0.0005$.

Numerical Simulations Continue.....

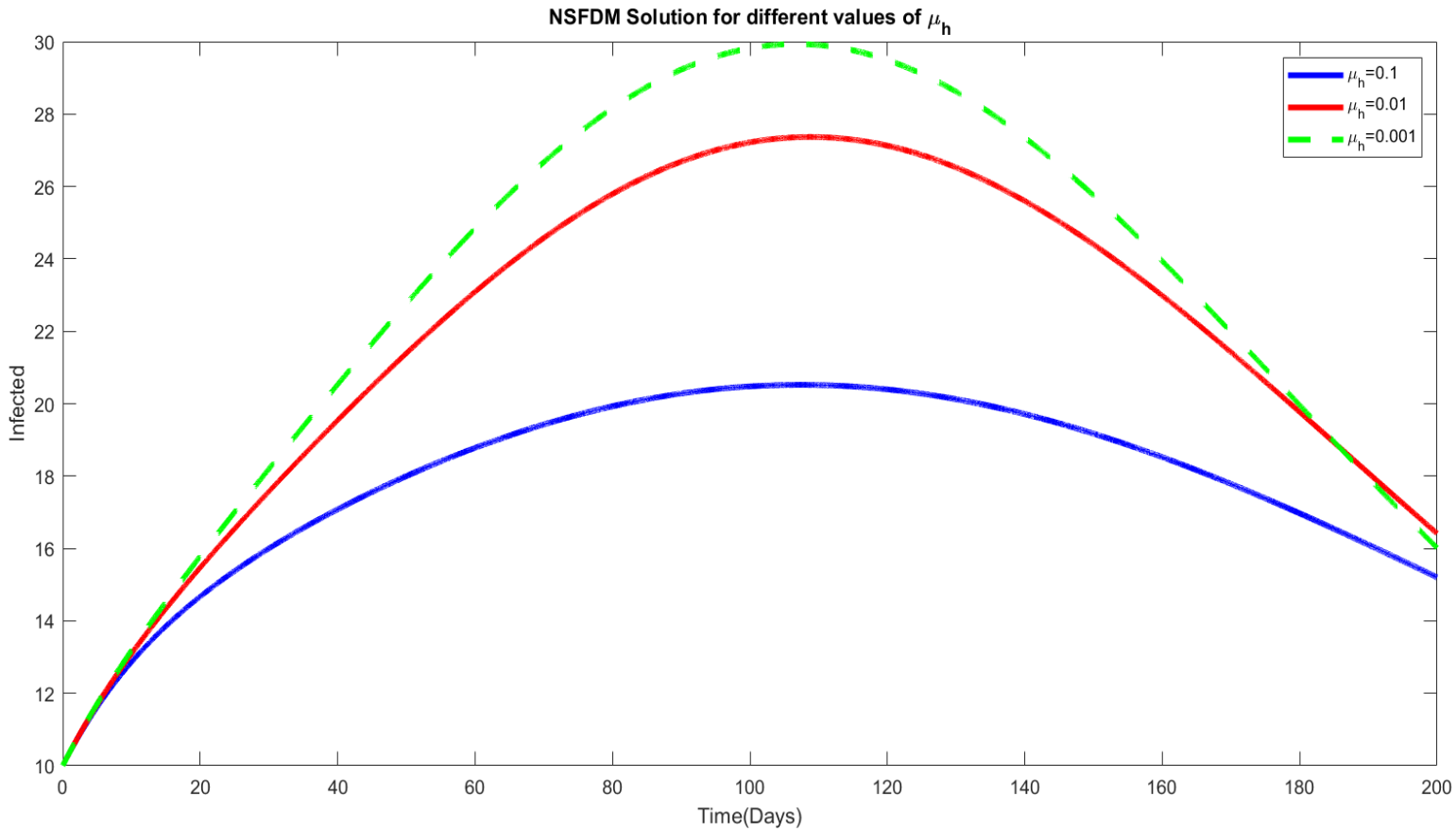

Figure 8: Shows evolution of infected individuals for different values μ_h : $\mu_h = 0.1, \mu_h = 0.01$ and $\mu_h = 0.001$.

Numerical Simulations Continue.....

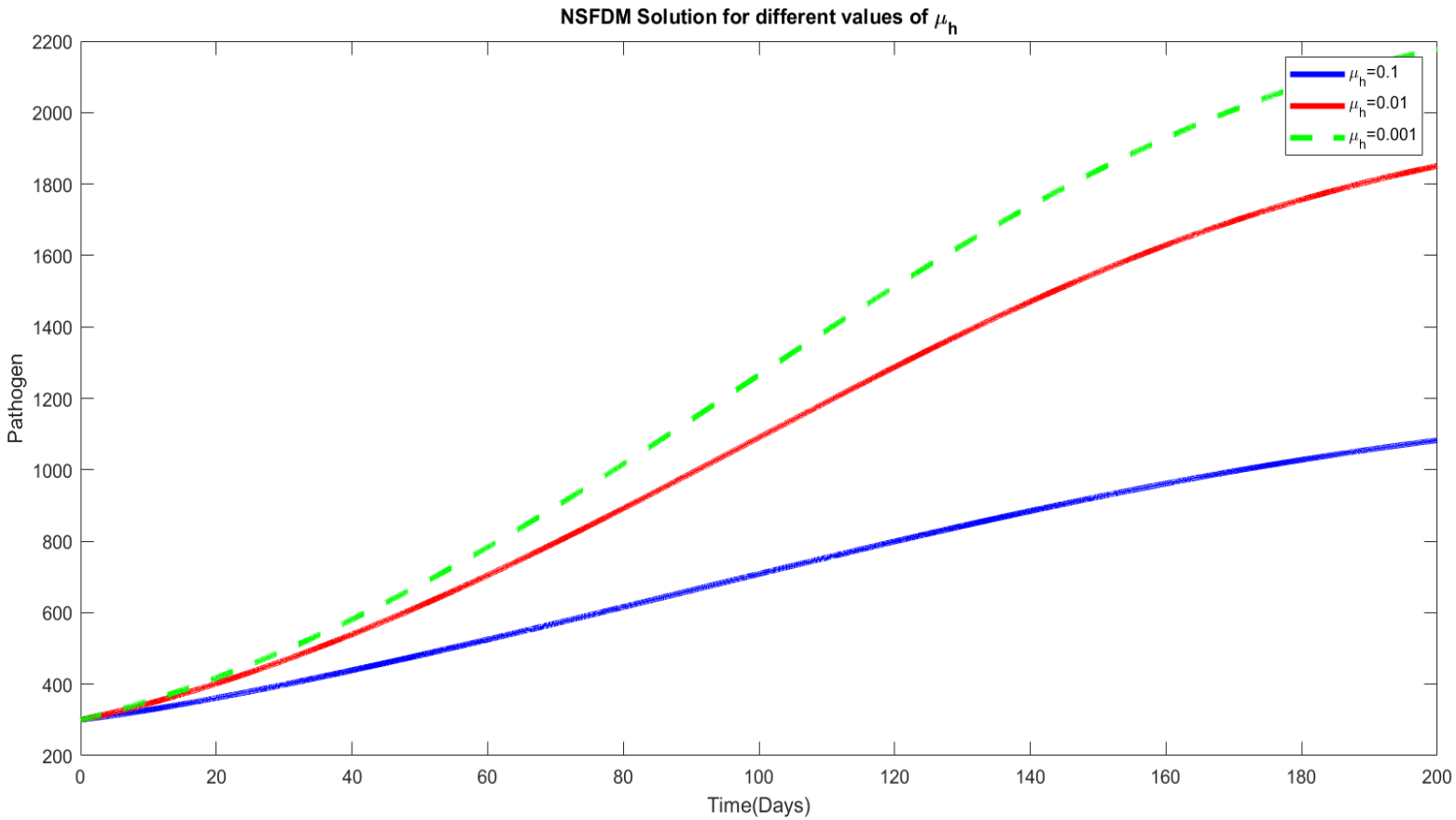

Figure 9: Shows evolution of pathogen in the environment for different values μ_h : $\mu_h = 0.1, \mu_h = 0.01$ and $\mu_h = 0.001$.

Numerical Simulations Continue.....

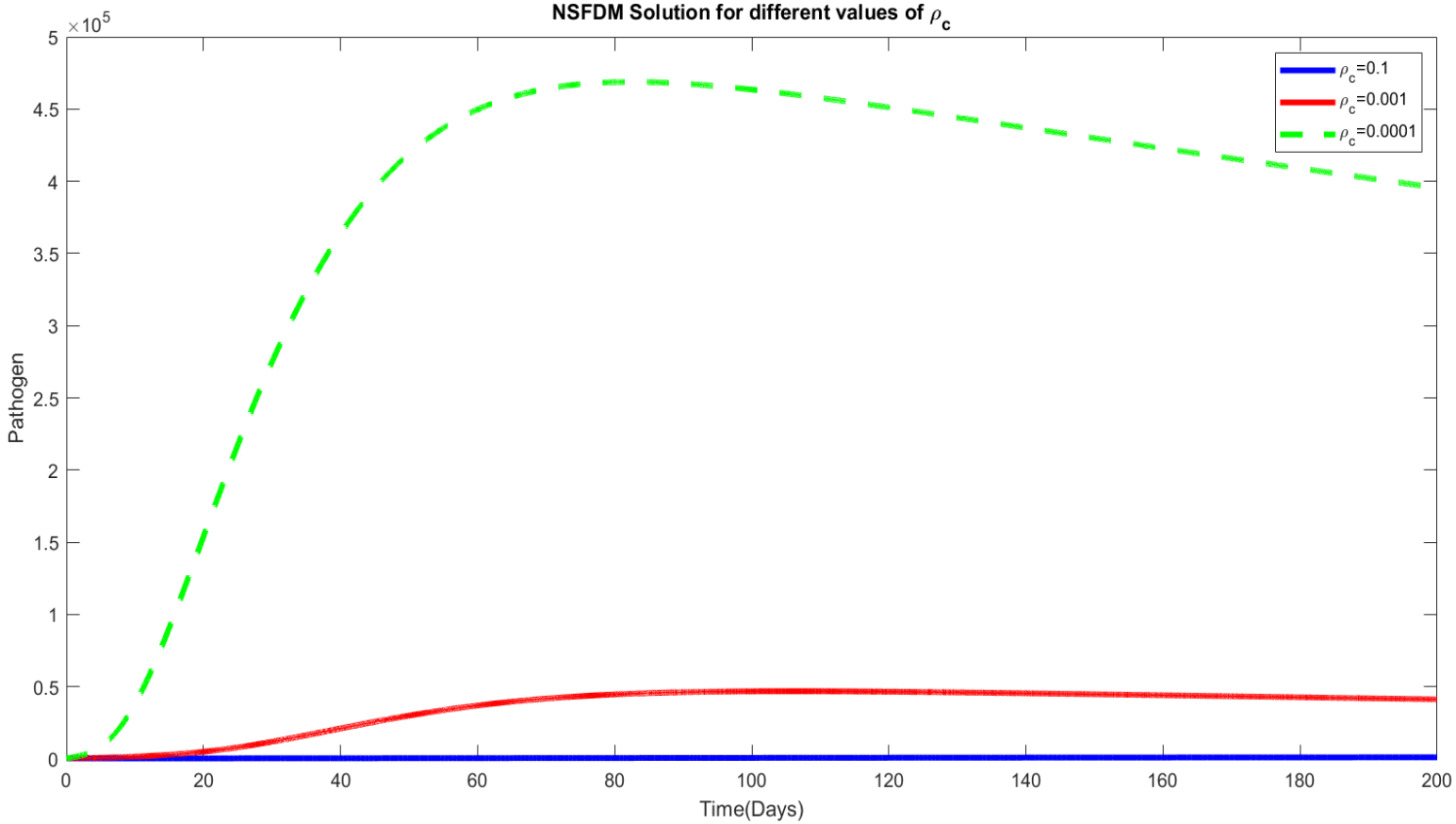

Figure 10: Shows evolution of pathogen in the environment for different values ρ_c : $\rho_c = 0.0001, \rho_c = 0.001$ and $\rho_c = 0.1$.

Numerical Simulations Continue.....

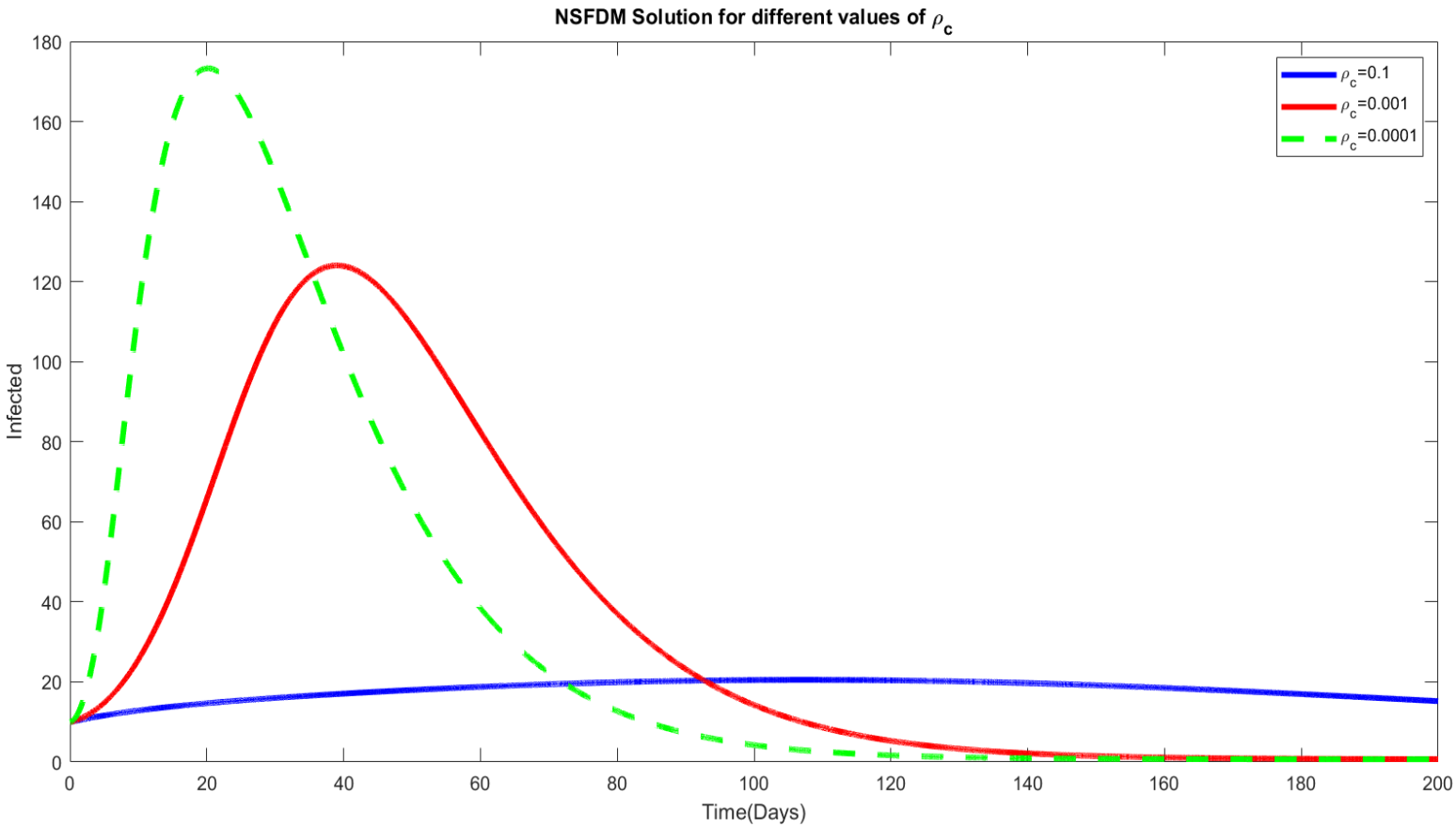

Figure 11: Shows evolution of S_H, I_H and V_H for different values ρ_c : $\rho_c = 0.0001, \rho_c = 0.001$ and $\rho_c = 0.1$.

Numerical Simulations Continue.....

- The results in figure 4 and 5 show that the infected and pathogen populations increase to the maximum until they reach their equilibrium level when viral replication rate at the site of infection increases, The results show that any action that can slow down the replication rate will be effective in reducing the number of *norovirus* infections among human community.
- The results in figure 6 and 7 show that the infected and pathogen populations increase to the maximum until they reach their equilibrium level when the shedding rate by infected individual increases. The results show that any action that can hinder the shedding rate will be effective in reducing the number of *norovirus* infections among human community.
- The results in figure 8 and 9 show that the infected and pathogen populations decrease when the natural death rate of virus within an infected individual increases. The results show that any action that can kill the pathogens within an infeted individual will be effective.

Numerical Simulations Continue.....

- The results in figure 10 and 11 show that the pathogen and infected populations decrease when immune cells activation increases. The results show that any measure to increase immune activation will be effective in reducing the number of *norovirus* infections among human community.
- Therefore we conclude that microscale dynamics has great influence on disease progression and hence cannot be ignored in way to combat the infetions.

Conclusion:

- Once the minimum infectious dose is consumed, then the infection at the microscale is sustained by pathogen replication.
- The reduction of the dimension in order of full nested multiscale model enable us to estimate a composite parameter, $\widehat{N_h}$, which is difficult to estimate using single-scale modelling approach.
- All the microscale parameters varied, have an influence on macroscale variables.
- Therefore we conclude that microscale dynamics has great influence on disease progression and hence cannot be ignored in way to combat the infetions.

References

- Dai, J., Dan, W., Li, N., Wang, R., Zhang, Y., Li, N., ... & Wang, J. (2018). Synthesis and antibacterial activity of C2 or C5 modified and D ring rejiggered canthin-6-one analogues. Food chemistry, 253, 211-220.
- Garira, W., & Mathebula, D. (2019). A coupled multiscale model to guide malaria control and elimination. *Journal of theoretical biology*, 475, 34-59.
- Gaythorpe, K. A. M., Trotter, C. L., Lopman, B., Steele, M., & Conlan, A. J. K. (2018). Norovirus transmission dynamics: a modelling review. Epidemiology & Infection, 146(2), 147-158.
- Jang, J., Hur, H. G., Sadowsky, M. J., Byappanahalli, M. N., Yan, T., & Ishii, S. (2017). Environmental Escherichia coli: ecology and public health implications—a review. Journal of applied microbiology, 123(3), 570-581.
- Bányai, K., Estes, M. K., Martella, V., & Parashar, U. D. (2018). Viral gastroenteritis. *The Lancet*, 392(10142), 175-186.

- Pastor-Satorras, R., Castellano, C., Van Mieghem, P., & Vespignani, A. (2015). Epidemic processes in complex networks. Reviews of Modern Physics, 87(3), 925.
- Mathebula, D. (2018). Multi-Scale Modelling of Vector-Borne Diseases (Doctoral dissertation).
- Netshikweta, R., & Garira, W. (2017). A multiscale model for the world's first parasitic disease targeted for eradication: guinea worm disease. *Computational and Mathematical Methods in Medicine*, 2017.
- Garira, W. (2019). The Replication-transmission Relativity theory for Multiscale Modelling of infectious Disease Systems. *Scientific Reports*, 9(1), 1-17.
- Simmons, K., Gambhir, M., Leon, J., & Lopman, B. (2013). Duration of immunity to norovirus gastroenteritis. *Emerging Infectious Diseases*, 19(8), 1260.
- Van den Driessche, P., & Watmough, J. (2002). Reproduction numbers and sub-threshold endemic equilibria for compartmental models of disease transmission. *Mathematical Biosciences*, 180(1-2),

THANK YOU